An Examination of the Systematic Properties of Source Lists for WFPC2 and ACS Derived from DAOphot

Michael A. Wolfe and Stefano Casertano

ABSTRACT

The study of the systematic properties of source lists that have been generated via a reduction pipeline within the Hubble Legacy Archive can disclose how satisfactorily the source lists are constructed. If the source lists are created in a robust and consistent manner then the investigation of the systematic properties of source lists can be done by removing astrometric and rotational offsets to reveal any detector characteristics that might arise. This can be explored through the various residuals that remain after subtraction of the aforementioned offsets. Furthermore, prior to the removal of the rotational offsets numerous plots can give qualitative information as to whether there is a large or small angle offset that is to be removed. This information can be inferred from the distribution of data points and the slopes correlated with these distributions. Moreover, after the removal of these offsets and looking at the data from an overall view point instead of on an individual basis, information can be derived that point to charge transfer efficiency, throughput, sensitivity, and quantum efficiency losses. Also, it is possible to detect any problems with calibration files if the source of the anomaly is not tied to any detector characteristics. The derivation of this information can only be the aftermath of a consistent and appropriate derivation of each individual source list.

1. Introduction

The examination of systematic properties is an important step in producing a product that is robust in all aspects when that product is repeatedly demanded by a group of people. Therefore, this examination is essential in the production of source lists that are generated through the Hubble Legacy Archive (HLA) from Hubble Space Telescope (HST) photometric observations[1]. The exploration of the systematic properties of source lists can also expose any errors or non-optimal parameter values that go into source list generation. The source lists are created from a pipeline that uses DAOphot and Source Extractor (SExtractor; Bertin & Arnouts 1996) to calculate

---

[1] Based on observations made with the NASA/ESA Hubble Space Telescope, and obtained from the Hubble Legacy Archive, which is a collaboration between the Space Telescope Science Institute (STScI/NASA), the Space Telescope European Coordinating Facility (ST-ECF/ESA) and the Canadian Astronomy Data Centre (CADC/NRC/CSA).

astrometry and fluxes. Note that the version of DAOphot used is an IRAF[2] implementation, not Peter Stetson's original program (Stetson 1987). The fluxes derived from DAOphot and SExtractor are subsequently used to generate magnitudes in the AB magnitude system (Oke & Gunn 1983). In order to perform a systematic examination pertaining to HLA source lists we assembled a catalogue of observations that cover an overlapping field of view (FOV), are separated in time, and done in several different filters. From these source lists we have matched, via right ascension and declination, objects found in the two source lists, hereafter referred to as paired source lists. Paired source lists refer to two source lists where one is designated the reference source list and the other is the compared source list. Note, however, that if there is more than one compared source list (and this is generally the case) with regards to a reference source list then paired source lists only refer to the reference source list and only one compared source list. No source lists that are designated as compared source lists are paired.

After astrometric offsets have been derived and removed, matches between the paired source lists are determined. After the matches have been ascertained rotations (if any and however small) have been removed as well. We will step through each modification and show via plots and tabular information the knowledge that can be inferred from the current data sets. The paired source lists employed in this analysis were observed with Wide Field Planetary Camera 2 (WFPC2; 79 paired source lists) and Advanced Camera for Surveys (ACS; 8 paired source lists) using mainly the F606W and F814W filters. The source lists will be compared and analyzed after the astrometric offsets have been removed and with and without rotation. Furthermore, outliers have been identified and analyzed to determine if the cause is due to DAOphot or SExtractor or if there are anomalies in the exposures themselves. See Wolfe & Castertano 2011a for an analysis showing that the outliers originate in the single and final drizzled images and not from the HLA pipeline. In order to facilitate the examination of the systematic properties of HLA source lists several Interactive Data Language (IDL) programs were written and adopted to analyze paired source lists.

2. The Data

The pipeline that generates the source lists outputs a text file that has a header and numerous columns. The header contains information regarding observational parameters and numerous quantitative and qualitative values produced during the derivation of source lists by DAOphot, *i.e.,* data quality flags, aperture correction, processing dates, whether the charge transfer efficiency (CTE) correction was done, and the Modified Julian Date (MJD) used in calculating the CTE. The main body of the source list has columns that pertain to astrometry, identification numbers, photometry (aperture and CTE corrected magnitudes), sky values, fluxes, concentration indexes, data quality flags, and CTE values. The range of the data covers roughly 8 years, from: January

---

[2]IRAF is distributed by the National Optical Astronomy Observatory, which is operated by Associations of Universities for Research in Astronomy, Inc., under cooperative agreement with the National Science Foundation.

23, 1996 through April 18, 2004. There were numerous filters used and these are: F300W, F336W, F410M, F450W, F467M, F547M, F555W, F606W, F675W, F702W, and F814W. However, the most frequent filters used in this analysis are F606W and F814W.

Throughout the rest of this document source lists will be designated first by proposal number and secondly by the visit identification, e.g., 08048_02 and 05941_04. When the source lists are compared the one with the most recent date of observation is employed as a reference, while all other source lists, which of course, possess the same field of view and filter, are considered to be the comparison source lists. The source lists used in this analysis were required to have the same FOV with a leeway of $10''$ because pointings in each of the exposures used to create the source lists will not be exactly the same. This is a consequence of using exposures that come from various proposals and times. As a final requirement only paired source lists with more than 50 matches are used in the analysis, as this number is adequate for a robust measure of offsets, angles, and slopes.

3. Part I: Individual Source List Comparison Results

3.1. Astrometric Offset

The astrometric offset is determined using the idl software match_dao_cat.pro, which reads in the source lists and then finds offsets by taking the right ascensions and declinations contained within the reference source list and subtracting every entry found in the comparison source list. The differences are put into differential right ascension and differential declination bins and the bin containing the most counts is then used as the offset that is then subtracted from the right ascensions and declinations found in the reference source list. Before relating the information provided by analyzing numerous right ascension and declination plots it will be important to explain what the four plots are in Figures 1, 3, 5, and 7. The first figure (upper left) has a plot of differential right ascension vs. right ascension and the second figure (upper right) is a plot of differential declination vs. declination. The bottom two plots are differential declination vs. right ascension (left) and differential right ascension vs. declination (right). Figures 1, 3, 5, and 7 show that the astrometric offset has been removed leaving only the rotational offset.

3.2. With Rotation

In this section we will compare and analyze paired source lists that still have a rotational offset in right ascension and declination. At this stage we can determine if there is any residual offset that has not been taken out of the right ascension and declination. We find in the top left and right of Figure 1, which is a comparison between 08048_02 and 05941_04, shows distinct non-random distributions that signify a substantial rotation between the two source lists. In the bottom left and right plots of Figure 1, it is shown that there is a correlation between the slopes and that

3

they are negatives of each other. This behavior signifies that there is a significant rotation between the two source lists being compared. Demonstration of rotations between paired source lists can also be discerned from vector plots. A vector plot is a plot in which pairs of points are drawn as vectors. If there is a significant rotation between paired source lists then when the vectors are drawn, all or a majority vectors will distribute themselves in a circular fashion. This is because the rotation between the two source lists offsets the right ascension and declination in the same direction. The vectors will increase in size from the center of the FOV as well and is a result of the arc lengths ($s = r\theta$) increasing as vectors are displaced from the center of the FOV. This behavior manifests itself as a rotational vector field, which is shown in Figure 2. The size of the vectors and the rotational distribution of the vectors depends on the magnitude of the rotational offset. Therefore, it is clear from the vector field in Figure 2 (comparison between 08048_02 and 05941_04) that there is a significant rotational offset that has to be removed. In contrast, the comparison between 08048_02 and 07274_04, as shown in Figure 3, depicts a random distribution in the top two plots. Moreover, these random distributions display slopes that are both positive and the bottom two plots show small slopes that have opposite signs, but this represents a modest rotational offset. Inspection of Figure 4 confirms that there is essentially no rotational offset as the vectors point in random directions as opposed to the rotation displayed by the vectors in Figure 2.
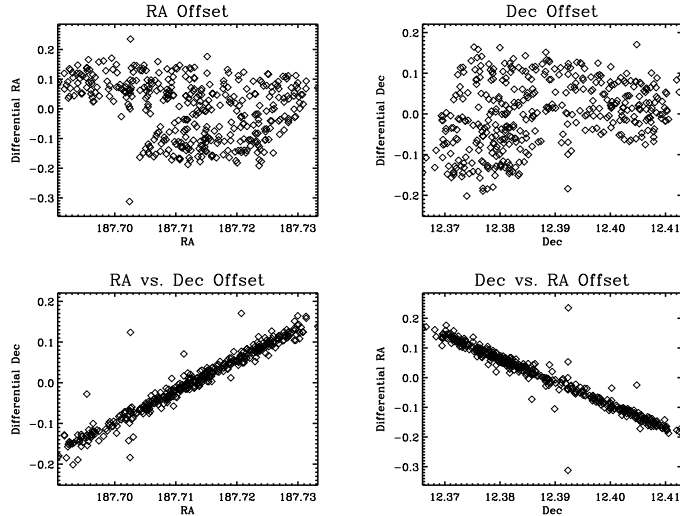

Fig. 1.— The two upper plots show that there is a distinct non-random distribution. The two lower panels show slopes that are negatives of each other and this reveals that there is a significant rotation. The abscissas are in decimal degrees and the ordinates are in arcsec. The source lists compared are 08048_02 and 05941_04.

4
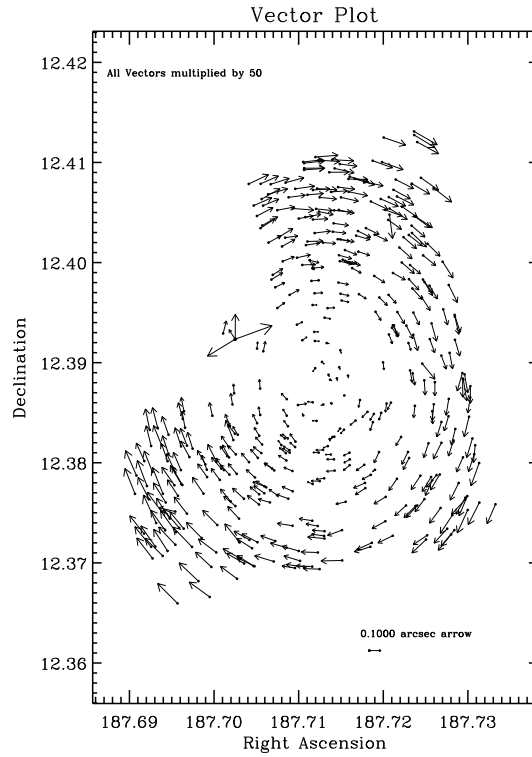
Fig. 2.— This vector field plot shows that there is a considerable rotation to be removed from the source lists being compared. The amount of rotational offset can be found Table 1. The abscissas and ordinates are in decimal degrees. The source lists compared are 08048_02 and 05941_04. Note that all vectors are multiplied by 50 to enhance the vector field.
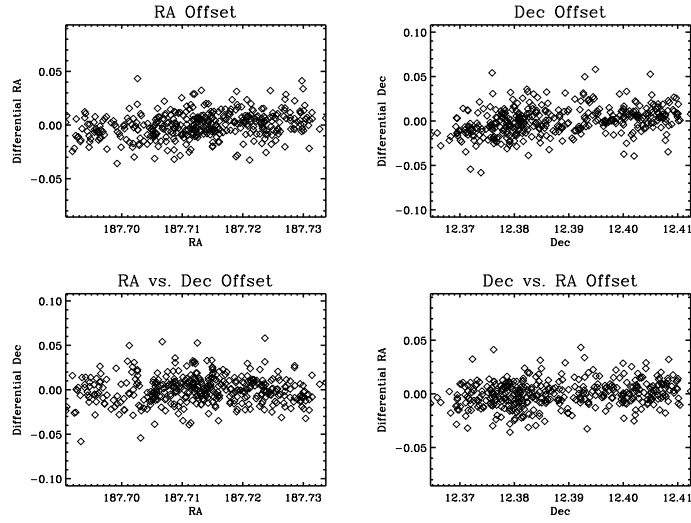
Fig. 3.— The two upper plots show that there is a random distribution in the data around zero, however, there does appear to be slopes in each distribution. The two lower panels show limited slopes that are negatives of each other, which represents a modest rotation. The slopes in the top and bottom plots are used to measure different parameters (see Section 3.3) associated with the paired source lists and therefore will have different values. The abscissas are in decimal degrees and the ordinates are in arcsec. The source lists compared are 08048_02 and 07274_04.
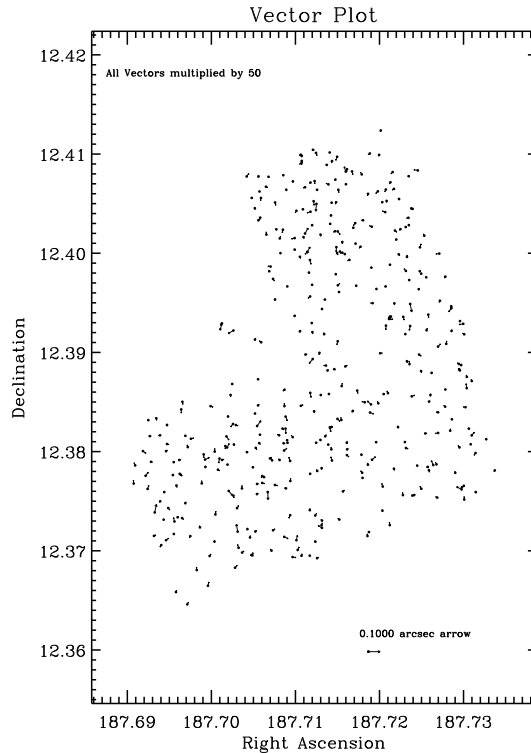
Fig. 4.— This vector field plot does not reveal a rotation between the two source lists being compared. The abscissas and ordinates are in decimal degrees. The source lists being compared are 08048_02 and 07274_04. Note that all vectors are multiplied by 50 to enhance the vector field.

3.3. Without Rotation

In this section we continue our analysis and comparison of source lists, however, in these cases the rotational offsets has been removed. In order to remove the rotational offsets the right ascension and declination of both source lists are mapped to each other. A least squares fit is used to map from one source list to another and the three angles that are derived give the best fit for the transformation. Additionally, in this transformation no small angle approximations were undertaken. The rotation was then removed from the second source list (not the reference source list). Table 1 has the astrometric and rotational offsets that were removed from all of the paired source lists and the RMSs of the differential right ascension and differential declination after the astrometric and rotational offsets have been removed. Table 1 has the columns: instruments used to generate the source lists, data sets compared, dates of the observations, Δright ascension (differential right ascension) and standard deviations, Δdeclination (differential declination) and standard deviations, rotational offsets, Δright ascension and Δdeclination RMSs and filter used

7

in the observations. Now that both offsets have been removed any remaining residuals should be related to the detector characteristics. Since we have source lists that span several years we can determine how the detector changes with time, if at all.

Before proceeding to make comparisons of the various figures it is important to describe what potential detector characteristics can be determined from the residuals after removing astrometric and rotational offsets. For starters, if the two top plots (differential right ascension vs right ascension and differential declination vs declination, left and right top plots, respectively) have slopes that are of the same sign then this is an indication of a change in plate scale. This change in plate scale can be calculated to within an order of magnitude by obtaining the average of both slopes. Moreover, if the slopes are of opposite signs of each other then the detector characteristic that can be approximated is a type of skew. The skew in this case represents different plate scales for right ascension and declination and is derived by calculating the difference in the slopes. For the bottom two plots (differential declination vs right ascension and differential right ascension vs declination, left and right bottom plots, respectively) if the slopes are the same then this is a measure of another type of skew, but in this case it is a measure of how much deviation there is from perpendicularity between the axes within each individual source list. This particular skew is estimated by computing the average of both slopes. If, however, the slopes are of opposite sign then this means that there still remains a rotational offset.

To begin, compare the two upper plots of Figures 1 and 5 and notice that the non-random distribution in Figure 1 has been replaced with a random distribution about zero. Furthermore, note that in the two lower plots in Figure 5 the slopes have disappeared and plots now show a random distribution about zero. Both of these pieces of evidence confirm that rotation has been mitigated. Additionally, comparison of Figures 2 and 6 reveal also that the rotation has indeed been removed as the rotational distribution of the vectors seen in Figure 2 has been replaced with a random distribution of vectors in Figure 6. Investigation of Figure 3 illuminates that there are slopes associated with the two upper plots as well as small but opposite slopes manifested in the two lower plots. Contrasting Figure 3 with Figure 7 shows that the rotational offset has been removed because the slopes in the bottom plots are approximately the same and have the same signs. Inspection of the top plots of Figures 3 and 7 show essentially no difference after the removal of rotational offsets, which implies that the slopes exhibited are possibly due to changing detector characteristics as the observations span about 6 years for the source lists 08048_02 and 05941_04 and approximately 3 years for the paired source lists 08048_02 and 07274_04. Figures 4 and 8 both show no rotational vectors but do display random vectors, which implies that there is no apparent rotational offset between the paired source lists 08048_02 and 07274_04. However, in Figure 3 small opposite signed slopes appear in the bottom two plots. This means that the vector plots along with Figure 3's bottom plots should be used in conjunction to verify a rotational offset. Also in Figure 7 in the upper right plot there is a gap in the data at a declination of ≈ 12.392 and curves towards smaller values of declination. This same gap is also present in the lower left plot at a right ascension of ≈ 187.704 and curves toward smaller values of right ascension.

The change in plate scale and a measurement of both types of skews can be found in Table 2. Note that in the plots the slopes have units of arcsecs/degree ($''/\circ$) and the resultant plate scale changes and skews have been divided by $3600''$. Consequently the units now divide out ($\circ/\circ$) and only a number is left. The columns of Table 2 are: data sets compared, Δplate scale, skew (plate skew), and skew (perpendicularity between axis). By comparing to the slopes found from other paired source lists it has been determined that the slope values found in the two paired source lists analyzed in this document are representative of the entire set of paired source lists. Furthermore, the small values presented in Table 2 imply that the plate scale of WFPC2 has changed insignificantly over time and that both skews have little consequence after astrometric and rotational offsets have been expunged. The axis skew should be small as the data were taken at a low value for the declination. As the declination increases the right ascension arcs become smaller and is related to the declination through the $\cos(\delta)$ factor used in calculating the right ascension arcs. When the declination increases and the right ascension arcs decrease this imparts a non-perpendicularity between the two axes within the individual source lists. Additionally, the FOV of the observations will show a miniscule effect of non-perpendicularity as the ranges for right ascension and declination are small. Mathematical derivations for Δplate scale, plate scale skew, and rotation can be found in the Appendix.
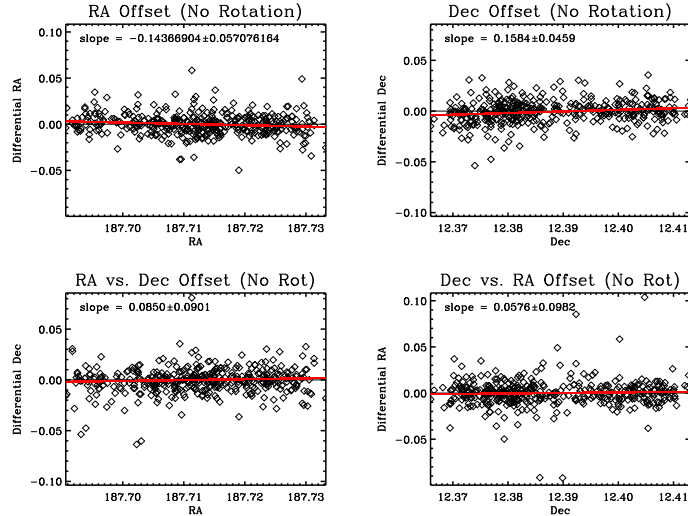
Fig. 5.— The two upper plots show that the distinct non-random distribution has been removed. The two lower panels show a random distribution with slopes of the same sign, which clearly indicates that the rotation has been removed. The red line is a least-square polynomial fit to the data. The abscissas are in decimal degrees and the ordinates are in arcsec. The source lists compared are 08048_02 and 05941_04.
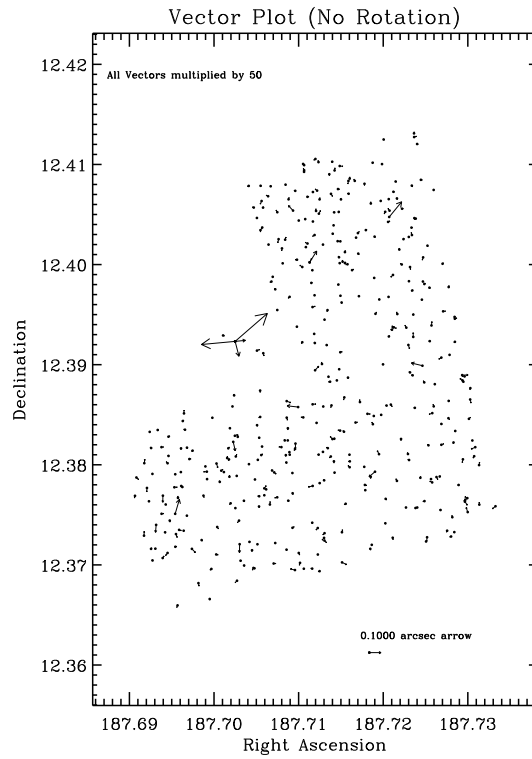
Fig. 6.— This vector field plot shows that the rotation has been removed from the source lists being compared. The abscissas and ordinates are in decimal degrees. The source lists compared are 08048_02 and 05941_04. Note that all vectors are multiplied by 50 enhance the vector field.
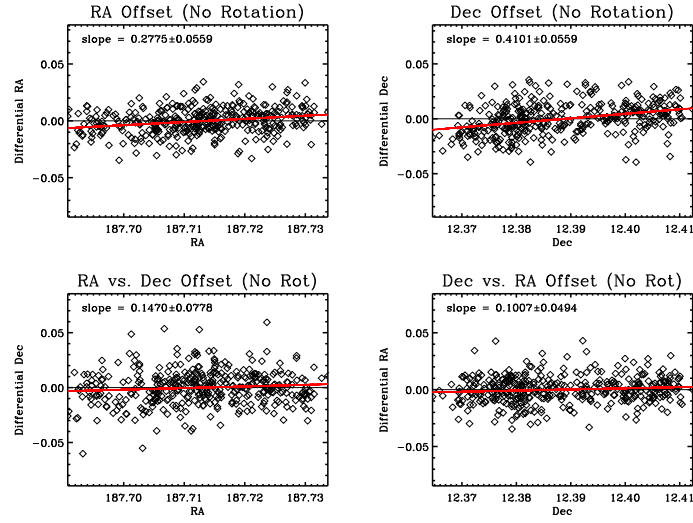
Fig. 7.— The upper left plot reveals positive slopes in both plots that still remain after astrometric and rotational offsets have been removed. The two lower panels show a random distribution that have slopes of the same sign, which clearly indicates that the rotation has been removed. The red line is a least-square polynomial fit to the data. The abscissas are in decimal degrees and the ordinates are in arcsec. The source lists compared are 08048_02 and 07274_04.
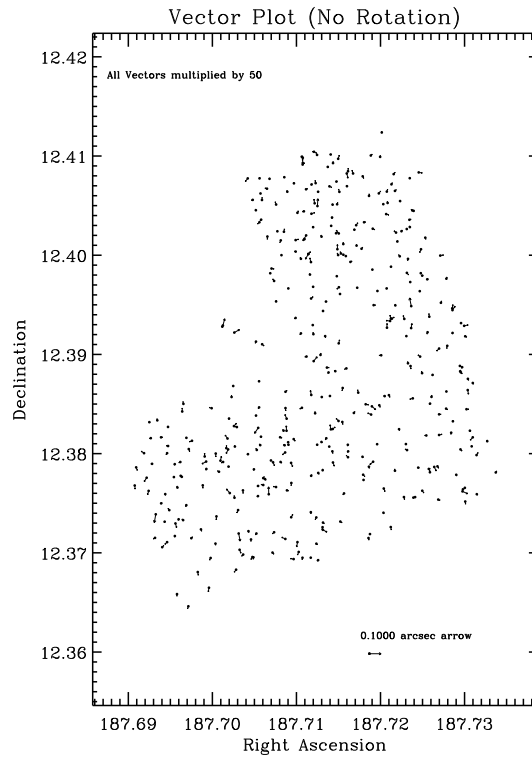
Fig. 8.— This vector field plot reveals relatively no change after the small rotation between the two source lists has been removed. The abscissas and ordinates are in decimal degrees. The source lists being compared are 08048_02 and 07274_04. Note that all vectors are multiplied by 50 to enhance the vector field.

Table 1: Offsets Between Source Lists and RMS

| Instr	Data Comp	Data Ref	Date Comp	Date Ref	ΔRA″	ΔRA″ Stddev	ΔDec″	ΔDec″ Stddev	ΔRot°	ΔRot° Error	ΔRA RMS″	ΔDec RMS″	Filter
acs	9438_01	9438_13	2003.0385	2004.0870	0.0099	0.0074	0.0059	0.0050	-0.0006	0.0059	0.0086	0.0050	f814w
acs	9438_01	9438_03	2003.0385	2003.0570	-0.0039	0.0177	-0.0019	0.0076	-0.0023	0.0024	0.0176	0.0073	f814w
acs	9438_02	9438_13	2003.0409	2004.0870	-0.0092	0.0076	0.0074	0.0047	0.0008	0.0058	0.0078	0.0052	f814w
acs	9438_02	9438_03	2003.0409	2003.0570	-0.0229	0.0166	-0.0001	0.0075	-0.0010	0.0024	0.0163	0.0075	f814w
acs	9438_03	9438_13	2003.0570	2004.0870	0.0156	0.0182	0.0061	0.0065	0.0011	0.0073	0.0180	0.0069	f814w
acs	9438_04	9438_05	2003.0517	2004.0793	-0.0108	0.0089	0.0071	0.0062	-0.0005	0.0022	0.0079	0.0062	f555w
acs	9811_01	9811_05	2004.2129	2004.2961	-0.0093	0.0066	0.0126	0.0060	0.0001	0.0080	0.0058	0.0065	f606w
acs	9811_04	9811_05	2004.2951	2004.2961	0.0153	0.0077	0.0183	0.0064	-0.0018	0.0084	0.0069	0.0057	f606w
wfcp	05477_0d	8048_02	1995.0879	2001.8732	0.0592	0.1145	-0.6723	0.0924	0.1402	0.0050	0.0247	0.0185	f814w
wfcp	05941_04	8048_02	1995.8881	2001.8732	0.1166	0.1018	-0.7473	0.0828	0.1238	0.0050	0.0250	0.0187	f814w
wfcp	06775_04	8048_02	1998.1485	2001.8732	-0.1554	0.0135	-0.5857	0.0142	-0.0029	0.0058	0.0129	0.0141	f814w
wfcp	07274_04	8048_02	1998.9564	2001.8732	-0.2496	0.0126	-0.3285	0.0158	-0.0018	0.0051	0.0122	0.0158	f814w
wfcp	08059_df	8059_dh	2000.6159	2000.6166	-0.0170	0.0568	-0.0027	0.0182	-0.0003	0.0026	0.0763	0.0229	f606w
wfcp2	6129_04	6129_05	1996.0479	1996.0644	-0.0573	0.0189	-0.0025	0.0182	0.0021	0.0132	0.0183	0.0184	f814w
wfcp2	6251_3u	7274_23	1995.5132	1999.4537	0.0164	0.1167	-0.0156	0.1005	0.1435	0.0084	0.0422	0.0324	f814w
wfcp2	6251_3v	7274_23	1995.5134	1999.4537	-0.0083	0.1228	-0.0067	0.0994	0.1446	0.0073	0.0492	0.0329	f814w
wfcp2	6251_3w	8090_if	1995.5138	1999.4533	0.0147	0.1179	0.0010	0.0970	0.1419	0.0067	0.0396	0.0260	f606w
wfcp2	6251_3x	8090_if	1995.5140	1999.4533	0.0296	0.1289	-0.0102	0.0972	0.1370	0.0066	0.0417	0.0540	f606w
wfcp2	6251_3z	7274_22	1995.5037	1999.4565	-0.0044	0.1203	-0.1094	0.0860	0.1427	0.0132	0.0135	0.0129	f814w
wfcp2	6251_40	7274_22	1995.5039	1999.4565	-0.0471	0.1261	0.0343	0.0859	0.1342	0.0131	0.0577	0.0227	f814w
wfcp2	6251_41	7274_22	1995.5041	1999.4565	0.0055	0.1223	0.0229	0.0931	0.1439	0.0135	0.0190	0.0221	f814w
wfcp2	6254_aa	6254_ac	1996.1622	1996.1625	3.4967	0.0147	-1.1875	0.0181	0.0000	0.0130	0.0130	0.0146	f814w
wfcp2	6254_ab	6254_ad	1996.1623	1996.1627	-0.4858	0.0160	0.0210	0.0192	-0.0002	0.0114	0.0158	0.0193	f606w
wfcp2	6254_bo	6254_bq	1996.4208	1996.4210	0.1464	0.0275	-0.5284	0.0193	0.0004	0.0100	0.0364	0.0202	f814w
wfcp2	6802_7a	6802_7e	1997.4199	1997.4377	-0.2118	0.0236	-0.1060	0.0239	0.0001	0.0125	0.0208	0.0225	f814w
wfcp2	6802_7b	6802_7e	1997.4200	1997.4377	0.0263	0.0253	-0.3172	0.0260	-0.0050	0.0110	0.0271	0.0249	f814w
wfcp2	6802_7c	7909_jk	1997.4202	1998.3711	-0.0181	0.0233	0.0344	0.0244	-0.0018	0.0093	0.0234	0.0252	f606w
wfcp2	6802_7d	7909_jk	1997.4375	1998.3711	-0.0160	0.0223	0.1568	0.0216	-0.0022	0.0114	0.0222	0.0214	f606w
wfcp2	6802_7f	7909_jk	1997.4379	1998.3711	-0.3618	0.0278	0.0105	0.0270	0.0006	0.0120	0.0279	0.0255	f606w
wfcp2	6938_06	7629_05	1998.4949	1999.4241	0.0032	0.0127	-0.0036	0.0078	-0.0031	0.0032	0.0121	0.0080	f814w
wfcp2	7202_ry	7202_s1	1997.7348	1997.7354	-0.0833	0.0531	0.0044	0.0213	-0.0005	0.0024	0.1001	0.0339	f450w
wfcp2	7202_rz	7202_s0	1997.7350	1997.7352	0.0434	0.0397	0.0185	0.0179	-0.0001	0.0014	0.0603	0.0216	f814w
wfcp2	7505_22	7505_26	1998.1072	1999.0995	-0.0145	0.0219	-0.0119	0.0189	-0.0026	0.0140	0.0226	0.0189	f814w
wfcp2	7505_23	7505_26	1998.1289	1999.0995	-0.0114	0.0170	-0.0310	0.0186	-0.0006	0.0131	0.0172	0.0188	f814w
wfcp2	7505_24	7505_26	1998.1694	1999.0995	-0.0625	0.0206	-0.0977	0.0222	-0.0012	0.0128	0.0211	0.0222	f814w
wfcp2	7505_25	7505_26	1998.2165	1999.0995	-0.0130	0.0189	0.0024	0.0174	-0.0049	0.0136	0.0187	0.0171	f814w
wfcp2	7505_51	7505_57	1999.0813	2000.0981	0.0247	0.0164	-0.0039	0.0198	0.0054	0.0109	0.0145	0.0197	f814w
wfcp2	7505_52	7505_57	1999.0976	2000.0981	0.0009	0.0179	-0.0002	0.0171	0.0068	0.0119	0.0164	0.0173	f814w
wfcp2	7505_53	7505_57	1999.1173	2000.0981	0.0039	0.0183	0.0033	0.0170	0.0054	0.0106	0.0175	0.0168	f814w
wfcp2	7505_54	7505_57	1999.1374	2000.0981	-0.0129	0.0159	-0.0100	0.0193	0.0077	0.0151	0.0132	0.0186	f814w
wfcp2	7505_55	7505_57	1999.1556	2000.0981	0.0103	0.0169	-0.0069	0.0183	0.0071	0.0135	0.0148	0.0179	f814w
wfcp2	7505_56	7505_57	1999.1747	2000.0981	0.0115	0.0165	-0.0054	0.0163	0.0072	0.0112	0.0146	0.0163	f814w
wfcp2	7505_71	7505_77	1999.0815	2000.0942	0.0122	0.0128	-0.0221	0.0151	0.0034	0.0133	0.0127	0.0153	f814w
wfcp2	7505_72	7505_77	1999.0980	2000.0942	0.0587	0.0179	-0.0006	0.0138	0.0026	0.0118	0.0162	0.0135	f814w
wfcp2	8059_fq	9634_9k	2001.6381	2002.6175	1.6329	0.1047	0.3496	0.0167	0.0067	0.0107	0.1164	0.0227	f606w
wfcp2	8090_of	8805_m0	1999.7202	2000.7210	-0.0329	0.0193	0.0548	0.0233	0.0045	0.0076	0.0185	0.0217	f606w
wfcp2	8090_og	8805_m0	1999.7204	2000.7210	-0.0098	0.0236	0.0071	0.0229	0.0058	0.0078	0.0220	0.0235	f606w
wfcp2	8090_op	8805_m0	1999.7471	2000.7210	-0.0351	0.0205	-0.0325	0.0204	0.0056	0.0189	0.0207	0.0202	f606w
wfcp2	8090_oz	8805_m0	1999.7474	2000.7210	-0.0030	0.0210	0.0108	0.0224	0.0032	0.0080	0.0210	0.0226	f606w
wfcp2	8490_01	8654_02	1999.4484	2001.4185	-0.0090	0.0195	0.0250	0.0178	-0.0010	0.0015	0.0195	0.0176	f555w
wfcp2	8490_01	8654_02	1999.4482	2001.4185	-0.0096	0.0172	0.0249	0.0154	-0.0009	0.0012	0.0173	0.0154	f814w
wfcp2	8654_02	9342_02	2001.4185	2003.3960	-0.0185	0.0173	0.0222	0.0163	-0.0019	0.0015	0.0174	0.0161	f555w
wfcp2	8654_02	9342_02	2001.4185	2003.3961	-0.0204	0.0148	0.0220	0.0135	-0.0002	0.0076	0.0148	0.0132	f814w
wfcp2	8805_lz	8805_m0	2000.7208	2000.7210	-0.0378	0.0185	0.0131	0.0190	-0.0008	0.0081	0.0204	0.0186	f606w
wfcp2	8805_va	8805_vd	2001.1125	2001.1130	0.4398	0.0219	-0.3204	0.0202	-0.0041	0.0087	0.0210	0.0204	f606w
wfcp2	8805_vb	8805_vd	2001.1126	2001.1130	0.0027	0.0232	-0.0049	0.0216	-0.0019	0.0090	0.0232	0.0217	f606w
wfcp2	8805_vc	8805_vd	2001.1128	2001.1130	1.3323	0.0209	0.5157	0.0209	-0.0037	0.0088	0.0206	0.0210	f606w
wfcp2	8805_xp	10084_fh	2001.1569	2004.1622	-0.0303	0.0307	-0.0200	0.0282	0.0013	0.0103	0.0305	0.0311	f606w
wfcp2	9232_01	9342_02	2001.7473	2003.3961	-0.0663	0.0146	0.0442	0.0153	-0.0038	0.0038	0.0172	0.0166	f555w
wfcp2	9232_01	9342_02	2001.7471	2003.3960	-0.0678	0.0171	0.0459	0.0180	-0.0047	0.0036	0.0148	0.0147	f814w
wfcp2	9244_cj	10084_fh	2001.3013	2004.1622	-0.0106	0.0335	-0.0131	0.0283	-0.0023	0.0112	0.0365	0.0280	f606w
wfcp2	9244_q1	9244_q6	2001.7373	2001.7382	-0.9086	0.0198	-0.2323	0.0202	0.0009	0.0097	0.0198	0.0201	f606w
wfcp2	9244_q2	9244_q6	2001.7375	2001.7382	-0.6114	0.0187	0.0385	0.0217	0.0014	0.0099	0.0188	0.0212	f606w
wfcp2	9244_q3	9244_q6	2001.7377	2001.7382	-1.0054	0.0254	-0.3485	0.0278	0.0039	0.0096	0.0243	0.0265	f606w
wfcp2	9244_q4	9244_q6	2001.7378	2001.7382	-0.4785	0.0171	-0.0349	0.0183	-0.0011	0.0097	0.0172	0.0175	f606w
wfcp2	9244_q5	9244_q6	2001.7380	2001.7382	-0.7246	0.0209	-0.5266	0.0224	0.0008	0.0101	0.0213	0.0186	f606w
wfcp2	9244_s6	9709_xv	2001.7933	2003.9718	-0.0562	0.0198	-0.0153	0.0210	-0.0060	0.0098	0.0204	0.0208	f606w
wfcp2	9318_9x	10084_fh	2001.9931	2004.1622	0.0056	0.0287	-0.0229	0.0314	-0.0014	0.0106	0.0322	0.0366	f606w
wfcp2	9318_dv	10084_de	2002.0551	2004.1159	0.0747	0.0272	0.3305	0.0222	-0.0030	0.0108	0.0277	0.0231	f606w
wfcp2	9318_e0	10084_de	2002.0602	2004.1159	0.0726	0.0292	0.3702	0.0233	-0.0028	0.0107	0.0307	0.0257	f606w
wfcp2	9318_e1	10084_de	2002.0603	2004.1159	0.0817	0.0265	0.2466	0.0190	-0.0079	0.0111	0.0290	0.0237	f606w
wfcp2	9634_9j	9634_9k	2002.6172	2002.6175	1.4936	0.0905	0.2952	0.0181	0.0015	0.0102	0.1355	0.0207	f606w
wfcp2	9676_g2	9710_vt	2002.7190	2003.6395	0.4041	0.0720	-0.0664	0.0245	-0.0090	0.0039	0.1796	0.0521	f606w
wfcp2	9676_id	9709_r5	2002.7439	2003.7441	-0.0123	0.0200	0.0394	0.0197	-0.0036	0.0125	0.0191	0.0198	f606w
wfcp2	9676_je	9709_r5	2002.7565	2003.7441	0.0060	0.0278	0.1022	0.0236	-0.0061	0.0118	0.0272	0.0253	f606w
wfcp2	9676_qu	9709_r5	2003.7315	2003.7441	0.1125	0.0251	0.0690	0.0249	-0.0102	0.0124	0.0244	0.0228	f606w
wfcp2	9676_re	10084_fh	2002.7424	2004.1622	-0.0009	0.0286	-0.0025	0.0241	-0.0001	0.0110	0.0344	0.0245	f606w
wfcp2	9676_w8	10084_fh	2003.1607	2004.1622	-0.0033	0.0239	-0.0124	0.0208	-0.0031	0.0107	0.0238	0.0207	f606w
wfcp2	9677_l2	9677_m0	2002.6098	2002.6100	0.0109	0.0159	0.0095	0.0098	-0.0004	0.0035	0.0171	0.0097	f300w
wfcp2	9677_l2	9677_m0	2002.6098	2002.6100	0.0116	0.0164	0.0095	0.0103	-0.0003	0.0035	0.0185	0.0099	f606w
wfcp2	9677_l3	9677_m0	2002.6099	2002.6100	-0.0309	0.0194	0.0041	0.0125	-0.0017	0.0038	0.0238	0.0128	f300w
wfcp2	9677_l3	9677_m0	2002.6099	2002.6100	-0.0292	0.0188	0.0028	0.0127	-0.0014	0.0035	0.0219	0.0126	f606w
wfcp2	9677_tt	9710_vt	2002.7189	2003.6396	0.2115	0.0514	0.2346	0.0161	-0.0087	0.0042	0.0693	0.0222	f300w
wfcp2	9677_tt	9710_vt	2002.7189	2003.6395	0.2112	0.0497	0.2336	0.0181	-0.0089	0.0041	0.0804	0.0258	f606w
wfcp2	9709_a7	10084_fh	2003.2944	2004.1622	0.0206	0.0297	-0.0313	0.0295	0.0022	0.0125	0.0326	0.0299	f606w
wfcp2	9709_nh	9710_vt	2003.6395	2003.6395	0.3364	0.0548	-0.0754	0.0189	-0.0036	0.0036	0.1346	0.0361	f606w
wfpc2	8059_dd	8059_dh	2000.6166	2000.6214	-0.0091	0.0598	0.0068	0.0196	-0.0013	0.0026	0.0774	0.0239	f606w

Table 2: Plate Scale and Both Skews

Paired Source Lists	ΔPlate Scale	Skew (Plate Scale)[a]	Skew (Axis)[a]
08048_02, 05941_04	X	$8.391\pm2.034\times10^{-5}$	$1.981\pm3.701\times10^{-5}$
08048_02, 07274_04	$9.550\pm2.276\times10^{-5}$	X	$3.440\pm2.560\times10^{-5}$

[a] Skew definitions can be found in Section 3.3.

3.4. Differential Magnitudes

From the paired source lists differential magnitudes were calculated by subtracting the magnitudes associated with each match. Outliers are defined as being more than 3σ away from the mean differential magnitude and were eliminated. All means quoted are calculated after the outliers have been discarded. The source lists contain magnitudes derived from $0.10''$ and $0.30''$ aperture photometry and a total magnitude is provided as well. Figures 9 and 10 plot the differential magnitudes against magnitudes. In the plots are the overall mean values of the differential magnitudes and are shown as solid horizontal black lines, whose values along with RMSs are presented in Table 3. The columns of Table 3 are instrument used, data sets compared, dates when the observations were taken, $0.10''$ differential magnitudes and standard deviations, $0.30''$ differential magnitudes and standard deviations, and total magnitudes and standard deviations and filters of all paired source lists. The means, RMSs, and median errors can be found in the legend in the upper left corner. The magnitudes are placed into bins: the first bin has a range of four magnitudes to help ensure that there are enough points to derive robust statistics, the second and third bins are each one magnitude wide, while the last bin is set to have a variable width based upon the faintest magnitude present in the source list. These bin widths are shown as the first two numbers in the legend. The next two numbers are the number of data points in the bins and the first number is the number of data points after 3σ clipping, while the next number (in parenthesis) is the number of data points in the bin without 3σ clipping. The next two numbers are the means and RMSs in each particular bin. The last number is the median error in each magnitude bin. The vertical red bars are indicative of the median error in each magnitude bin. The small values of the overall mean shows that the aperture photometry is done properly and that DAOphot is producing reasonable fluxes. The number of cases where the $0.10''$ differential mean magnitudes are > 0.1 is 11 out of 81 or 13.6%. Moreover, the number of cases where the $0.30''$ mean differential magnitudes are > 0.1 is 5 out of 81 or 4.6%. These percentages are less than the percentages calculated for the same type of analysis when using SExtractor (Wolfe & Casertano 2011b).

Furthermore, this also shows that the matching of the two source lists is done in robust manner. Moreover, inspection of Figures 9 and 10 also reveals that the photometry is being produced correctly because the error and the scatter increase as objects become fainter.

14

Magnitude (0.10 arcsecs)

17.1 to 21.1: 13(14)pts, 0.0520±0.129, med err 0.010
21.1 to 22.1: 54(55)pts, 0.0364±0.086, med err 0.012
22.1 to 23.1: 115(118)pts, 0.0312±0.083, med err 0.016
23.1 to 24.6: 213(217)pts, 0.0344±0.081, med err 0.023

Magnitude (0.30 arcsecs)

16.2 to 20.2: 14(17)pts, 0.0479±0.078, med err 0.008
20.2 to 21.2: 69(72)pts, 0.0217±0.050, med err 0.012
21.2 to 22.2: 127(130)pts, 0.0267±0.043, med err 0.017
22.2 to 23.6: 182(185)pts, 0.0266±0.050, med err 0.020

Total Magnitudes

16.0 to 20.0: 3(6)pts, 0.0453±0.083, med err 0.020
20.0 to 21.0: 28(29)pts, 0.0248±0.067, med err 0.010
21.0 to 22.0: 174(180)pts, 0.0273±0.062, med err 0.020
22.0 to 23.5: 185(189)pts, 0.0262±0.061, med err 0.020

Fig. 9.— Shown in this figure are the differential magnitudes as a function of magnitude for 0.10″ and 0.30″ apertures and total magnitudes. The solid line represents the mean differential magnitude. The source lists compared are 08048_02 and 05941_04.
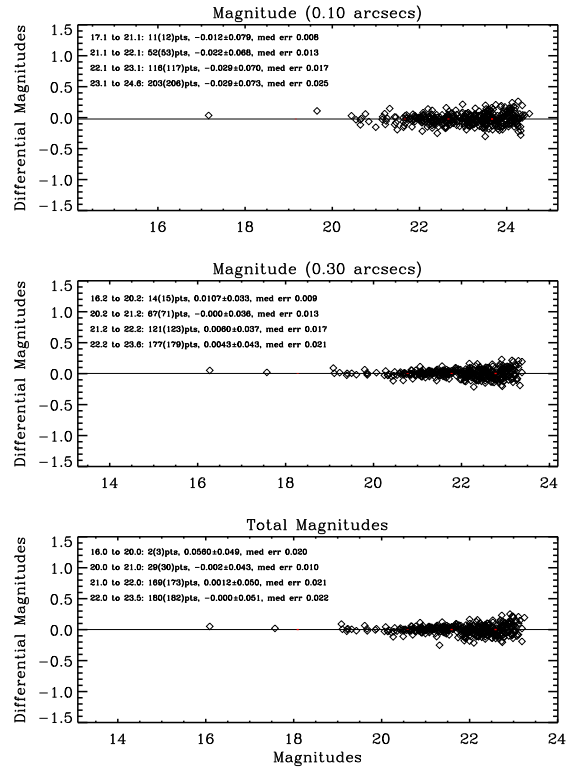
Fig. 10.— Shown in this figure are the differential magnitudes as a function of magnitude for 0.10″ and 0.30″ apertures and total magnitudes. The solid line represents the mean differential magnitude. The source lists compared are 08048_02 and 07274_04.

16

Table 3: Mean Differential Magnitudes

Instr	Data Comp	Data Ref	Date Comp	Date Ref	0.10″ Aper.	0.10″ Stddev	0.30″ Aper.	0.30″ Stddev	Total	Total Stddev	Filter
acs	9438_01	9438_13	2003.0385	2004.0870	0.0244	0.0753	0.0123	0.0337	0.0065	0.0355	f814w
acs	9438_01	9438_03	2003.0385	2003.0570	0.0012	0.1228	0.0011	0.0905	-0.0006	0.0949	f814w
acs	9438_02	9438_13	2003.0409	2004.0870	0.0150	0.0728	0.0087	0.0388	0.0043	0.0410	f814w
acs	9438_02	9438_03	2003.0409	2003.0570	0.0005	0.1037	0.0024	0.0921	-0.0007	0.0987	f814w
acs	9438_03	9438_13	2003.0570	2004.0870	0.0173	0.0952	0.0089	0.0334	0.0094	0.0417	f814w
acs	9438_04	9438_05	2003.0517	2004.0793	-0.0200	0.0930	-0.0160	0.0820	-0.0096	0.0838	f555w
acs	9811_01	9811_05	2004.2129	2004.2961	-0.0311	0.0870	-0.0195	0.0417	-0.0047	0.0432	f606w
acs	9811_04	9811_05	2004.2951	2004.2961	0.0189	0.0947	0.0021	0.0387	-0.0001	0.0474	f606w
wfcp2	05477_0d	08048_02	1995.0879	2001.8732	0.0505	0.1054	0.0358	0.0790	0.0347	0.0821	f814w
wfcp2	05941_04	08048_02	1995.8881	2001.8732	0.0434	0.0961	0.0276	0.0699	0.0285	0.0750	f814w
wfcp2	06775_04	08048_02	1998.1485	2001.8732	0.0191	0.0930	0.0147	0.0635	0.0135	0.0681	f814w
wfcp2	07274_04	08048_02	1998.9564	2001.8732	-0.0219	0.0892	0.0032	0.0688	0.0015	0.0740	f814w
wfcp2	08059_df	08059_dh	2000.6159	2000.6166	-0.0555	0.2325	-0.0382	0.1660	-0.0359	0.1705	f606w
wfcp2	6129_04	06129_05	1996.0479	1996.0644	0.0182	0.1568	-0.0398	0.1145	-0.0332	0.1135	f814w
wfcp2	6251_3u	07274_23	1995.5132	1999.4537	0.2337	0.1421	0.0934	0.1316	0.1251	0.1373	f814w
wfcp2	6251_3v	07274_23	1995.5134	1999.4537	0.1828	0.1360	0.0702	0.1057	0.0967	0.1276	f814w
wfcp2	6251_3w	08090_if	1995.5138	1999.4533	0.2276	0.1331	0.0615	0.1070	0.0853	0.1210	f606w
wfcp2	6251_3x	08090_if	1995.5140	1999.4533	0.2327	0.1324	0.0636	0.1011	0.0920	0.1231	f606w
wfcp2	6251_3z	07274_22	1995.5037	1999.4565	0.0388	0.1192	0.0153	0.0889	0.0405	0.1136	f814w
wfcp2	6251_40	07274_22	1995.5039	1999.4565	0.0351	0.0895	0.0302	0.0960	0.0324	0.1100	f814w
wfcp2	6251_41	07274_22	1995.5041	1999.4565	0.0529	0.1122	0.0200	0.0600	0.0200	0.0600	f814w
wfcp2	6254_aa	06254_ac	1996.1622	1996.1625	-0.0101	0.0816	-0.0132	0.1124	-0.0206	0.0884	f814w
wfcp2	6254_ab	06254_ad	1996.1623	1996.1627	0.0114	0.0920	0.0061	0.0784	0.0059	0.0842	f606w
wfcp2	6254_bo	06254_bq	1996.4208	1996.4210	0.0112	0.1755	0.0312	0.1860	0.0450	0.1776	f814w
wfcp2	6802_7a	06802_7e	1997.4199	1997.4377	-0.0114	0.0934	-0.0136	0.1059	-0.0061	0.1063	f814w
wfcp2	6802_7b	06802_7e	1997.4200	1997.4377	-0.0103	0.1020	0.0139	0.1807	0.0086	0.1550	f814w
wfcp2	6802_7c	07909_jk	1997.4202	1998.3711	0.0021	0.1182	-0.0089	0.1119	-0.0040	0.1150	f606w
wfcp2	6802_7d	07909_jk	1997.4375	1998.3711	0.0408	0.1164	0.0268	0.1211	0.0359	0.1348	f606w
wfcp2	6802_7f	07909_jk	1997.4379	1998.3711	0.0631	0.1488	0.0420	0.2082	0.0545	0.1938	f606w
wfcp2	6938_06	07629_05	1998.4949	1999.4241	0.0408	0.0680	-0.0612	0.0970	-0.0597	0.0972	f814w
wfcp2	7202_ry	07202_s1	1997.7348	1997.7354	-0.0157	0.2022	-0.0100	0.2868	-0.0131	0.2533	f450w
wfcp2	7202_rz	07202_s0	1997.7350	1997.7352	0.0025	0.1232	0.0026	0.2064	0.0038	0.1860	f814w
wfcp2	7505_22	07505_26	1998.1072	1999.0995	0.0629	0.1517	0.0209	0.1113	0.0194	0.1703	f814w
wfcp2	7505_23	07505_26	1998.1289	1999.0995	0.0729	0.1373	0.0103	0.1121	0.0304	0.1380	f814w
wfcp2	7505_24	07505_26	1998.1694	1999.0995	0.0720	0.1161	0.0203	0.1024	0.0341	0.1126	f814w
wfcp2	7505_25	07505_26	1998.2165	1999.0995	0.0806	0.1406	0.0020	0.0957	0.0236	0.1155	f814w
wfcp2	7505_51	07505_57	1999.0813	2000.0981	0.0279	0.1383	0.0166	0.1050	0.0143	0.1159	f814w
wfcp2	7505_52	07505_57	1999.0976	2000.0981	0.0586	0.1350	0.0234	0.0945	0.0342	0.1067	f814w
wfcp2	7505_53	07505_57	1999.1173	2000.0981	-0.0133	0.1170	0.0071	0.0994	0.0071	0.1067	f814w
wfcp2	7505_54	07505_57	1999.1374	2000.0981	0.0580	0.1475	0.0280	0.0932	0.0318	0.1320	f814w
wfcp2	7505_55	07505_57	1999.1556	2000.0981	0.0787	0.1448	0.0307	0.1013	0.0459	0.0982	f814w
wfcp2	7505_56	07505_57	1999.1747	2000.0981	0.0302	0.1179	0.0149	0.0977	0.0153	0.0886	f814w
wfcp2	7505_71	07505_77	1999.0815	2000.0942	-0.0582	0.1389	-0.0174	0.1072	-0.0139	0.1104	f814w
wfcp2	7505_72	07505_77	1999.0980	2000.0942	-0.0137	0.1304	-0.0061	0.1073	-0.0068	0.1055	f814w
wfcp2	8059_fq	09634_9k	2001.6381	2002.6175	-0.0309	0.1135	-0.0219	0.1059	-0.0237	0.1130	f606w
wfcp2	8090_of	08805_m0	1999.7202	2000.7210	-0.0061	0.1057	0.0081	0.1152	-0.0002	0.1126	f606w
wfcp2	8090_og	08805_m0	1999.7204	2000.7210	-0.0103	0.1069	0.0007	0.1219	0.0046	0.1161	f606w
wfcp2	8090_op	08805_m0	1999.7471	2000.7210	0.0120	0.1489	0.0087	0.1095	0.0150	0.1037	f606w
wfcp2	8090_oz	08805_m0	1999.7474	2000.7210	-0.0087	0.1171	0.0061	0.0989	0.0085	0.1001	f606w
wfcp2	8490_01	09342_02	1999.4484	2003.3960	0.0447	0.2377	0.0525	0.1803	0.0498	0.1858	f555w
wfcp2	8490_01	09342_02	1999.4482	2003.3961	-0.0240	0.0760	0.0214	0.0618	0.0170	0.0691	f814w
wfcp2	8654_02	09342_02	2001.4185	2003.3960	0.0067	0.1603	0.0019	0.1177	0.0001	0.1259	f555w
wfcp2	8654_02	09342_02	2001.4185	2003.3961	-0.0247	0.0627	-0.0006	0.0455	-0.0028	0.0505	f814w
wfcp2	8805_lz	08805_m0	2000.7208	2000.7210	0.0045	0.0988	-0.0038	0.1051	0.0073	0.0974	f606w
wfcp2	8805_va	08805_vd	2001.1125	2001.1130	-0.0149	0.1471	-0.0189	0.1309	-0.0137	0.1295	f606w
wfcp2	8805_vb	08805_vd	2001.1126	2001.1130	-0.0270	0.1183	-0.0184	0.1234	-0.0272	0.1199	f606w
wfcp2	8805_vc	08805_vd	2001.1128	2001.1130	-0.0272	0.1421	-0.0180	0.1255	-0.0180	0.1300	f606w
wfcp2	8805_xp	10084_fh	2001.1569	2004.1622	-0.2257	0.3373	-0.1335	0.2284	-0.1501	0.2593	f606w
wfcp2	9232_01	09342_02	2001.7473	2003.3961	0.0275	0.2236	-0.0053	0.1715	-0.0011	0.1795	f555w
wfcp2	9232_01	09342_02	2001.7471	2003.3960	0.0593	0.0990	0.0327	0.0825	0.0365	0.0909	f814w
wfcp2	9244_cj	10084_fh	2001.3013	2004.1622	-0.2862	0.3549	-0.1854	0.2320	-0.2052	0.2505	f606w
wfcp2	9244_q1	09244_q6	2001.7373	2001.7382	-0.0116	0.0950	-0.0116	0.1113	-0.0090	0.1129	f606w
wfcp2	9244_q2	09244_q6	2001.7375	2001.7382	-0.0042	0.1117	-0.0100	0.1082	-0.0118	0.1065	f606w
wfcp2	9244_q3	09244_q6	2001.7377	2001.7382	-0.0097	0.0970	-0.0016	0.1182	-0.0003	0.1108	f606w
wfcp2	9244_q4	09244_q6	2001.7378	2001.7382	0.0001	0.0927	-0.0051	0.1164	0.0063	0.1069	f606w
wfcp2	9244_q5	09244_q6	2001.7380	2001.7382	0.0052	0.0996	0.0044	0.1195	0.0127	0.1052	f606w
wfcp2	9244_s6	09709_xv	2001.7933	2003.9718	-0.1326	0.2938	-0.0761	0.1809	-0.0864	0.2056	f606w
wfcp2	9318_9x	10084_fh	2001.9931	2004.1622	-0.2493	0.3121	-0.1212	0.1919	-0.1402	0.2273	f606w
wfcp2	9318_dv	10084_de	2002.0551	2004.1159	0.0151	0.1775	-0.0006	0.1698	0.0012	0.1789	f606w
wfcp2	9318_e0	10084_de	2002.0602	2004.1159	0.0488	0.1269	0.0164	0.2020	0.0182	0.2092	f606w
wfcp2	9318_e1	10084_de	2002.0603	2004.1159	0.0222	0.1708	0.0165	0.1772	0.0203	0.1785	f606w
wfcp2	9634_9j	09634_9k	2002.6172	2002.6175	-0.0043	0.1064	-0.0145	0.1116	-0.0196	0.1115	f606w
wfcp2	9676_g2	09710_vt	2002.7190	2003.6395	0.0804	0.6053	-0.0960	0.2623	-0.0714	0.3125	f606w
wfcp2	9676_id	09709_r5	2002.7439	2003.7441	0.0546	0.1078	0.0181	0.1002	0.0311	0.0977	f606w
wfcp2	9676_je	09709_r5	2002.7565	2003.7441	0.0271	0.1319	-0.0158	0.1079	-0.0055	0.1278	f606w
wfcp2	9676_qu	09709_r5	2003.7315	2003.7441	0.0639	0.0923	0.0296	0.0846	0.0383	0.0811	f606w
wfcp2	9676_re	10084_fh	2002.9872	2004.1622	-0.0361	0.1852	-0.0509	0.1066	-0.0528	0.1357	f606w
wfcp2	9676_w8	10084_fh	2003.1607	2004.1622	0.0946	0.2373	0.0536	0.1356	0.0480	0.1482	f606w
wfcp2	9677_l2	09677_m0	2002.6098	2002.6100	0.0081	0.0635	0.0216	0.1328	0.0218	0.1197	f300w
wfcp2	9677_l2	09677_m0	2002.6098	2002.6100	-0.2796	0.2788	-0.1820	0.1765	-0.2050	0.2029	f606w
wfcp2	9677_l3	09677_m0	2002.6099	2002.6100	0.0506	0.0941	0.0254	0.1733	0.0247	0.1503	f300w
wfcp2	9677_l3	09677_m0	2002.6099	2002.6100	-0.3053	0.2968	-0.2185	0.1893	-0.2329	0.2143	f606w
wfcp2	9677_tt	09710_vt	2002.7189	2003.6396	0.0869	0.1450	-0.0309	0.1902	-0.0207	0.1676	f300w
wfcp2	9677_tt	09710_vt	2002.7189	2003.6395	0.0125	0.2546	-0.0432	0.1402	-0.0386	0.1562	f606w
wfcp2	9709_a7	10084_fh	2003.2944	2004.1622	0.1005	0.2367	0.0722	0.1789	0.0666	0.1758	f606w
wfcp2	9709_nh	09710_vt	2003.6395	2003.6395	0.0868	0.3069	-0.0222	0.1234	-0.0050	0.1589	f606w
wfpc2	08059_dd	08059_dh	2000.6166	2000.6214	-0.0908	0.3331	-0.0328	0.2384	-0.0431	0.2574	f606w

4. Part II: Overall Source List Comparison Results

4.1. Differential Astrometry

In this section we will explore the relationship between differential right ascension and differential declination as functions of each other and as a function of the date of the observations. In Figure 11 it is clear that most of the astrometric offsets are centered around zero with a range of 0.2″. Both Guide Star Catalog I (GSC I; Russell et al. 1990) and Guide Star Catalog II (GSC II; Lasker et al. 2008) have 3σ values of $\approx 2.0″$ and $\approx 0.7″$, respectively. The larger offsets ($\geq$ 0.2″ but $\leq 2.0″$) are reasonable because they fall within the 3σ of GSC I and GSC II. There is one outlier at a $\Delta RA \approx 3.4967$ and $\Delta Dec \approx$ -1.1875 and this outlier could be caused by poor registration of the astrometry with other database such as the Sloan Digital Sky Survey (SDSS; Pier et al. 2003), 2-Micron All Sky Survey (2MASS; Skrutskie et al. 2006), and GSC II during the multidrizzle process.

We examine a large offset that has been derived from the paired source lists 06254_ac and 06254_aa . The results can be found in Table 4 whose columns are: data sets compared in the first column, differential right ascension and differential declination in arcsecs and calculated with IDL in columns 2 and 3, while the last two columns are the same as 2 and 3 except for the offsets were calculated by hand using the right ascension and declination associated with each observation. It is readily apparent from the values in Table 4 that the calculations of the offsets from IDL and by hand are essentially the same. The small differences in the third and fourth decimal places can be attributed to differences in the precision in the right ascension and declination values derived from the HLA interface and the source lists derived from HLA. So it is not that these large offsets should be considered outliers, in the sense that there is an error but that the IDL software programs used are robust in deriving accurate astrometric offsets. Since there are no offsets that are greater than 10″ and since the leeway in matching FOVs is 10″ then this implies that robust astrometric offsets are being calculated.

Analysis of Figure 12 implies that there does not seem to be any correlation with time apparent in the data. In the top plot there does not seem to be any time difference dependence as all of the large offsets have time differences of 0 and 1, while for the smaller offsets the Δyear range is from 0 to ≈ 7 and are distributed around offsets of zero. The bottom plot shows essentially the same behavior except for the four larger differential declinations at time differences greater than 2.5. There does not appear to be any correlation with the negative offsets for the rest of the data points and this implies that there is no dependence on the time differences.
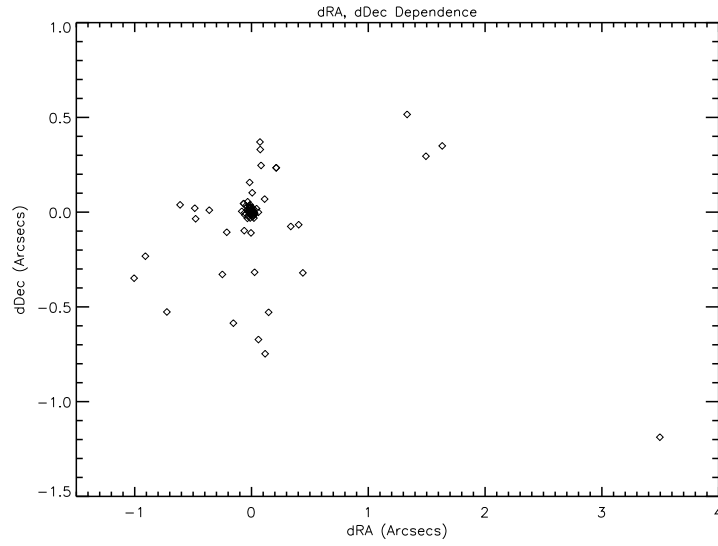
Fig. 11.— In this figure differential declination is plotted as a function of differential right ascension.
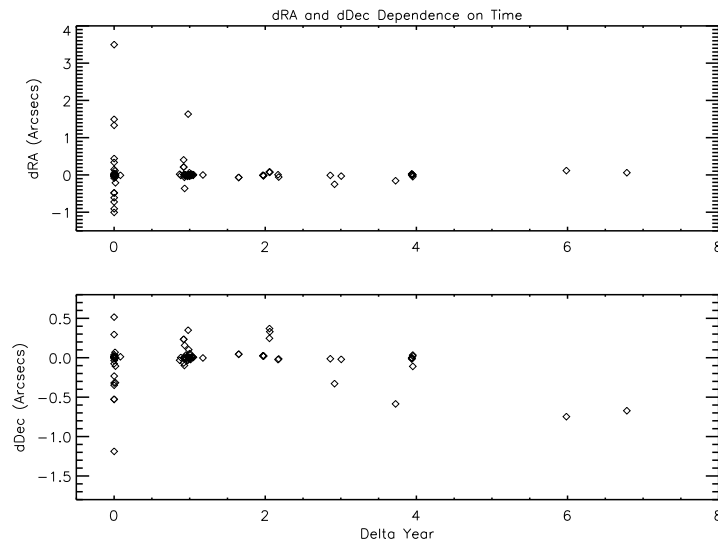
Fig. 12.— In this figure differential right ascension and differential declination are plotted as functions of Δyear. The Δyear values represent the differences in time of when the observations that went into generating two source lists were observed.

19

Table 4: Astrometric Offsets

Paired Source Lists	ΔRA (″, IDL)	ΔDec (″, IDL)	ΔRA (″, HLA)	ΔDec (″, HLA)
06254_ac, 06254_aa	3.4967	-1.1875	3.4945	-1.1800

4.2. Angles

As stated earlier rotational offsets were calculated and then removed from the source lists. All of the rotations derived from the paired source lists can be found in Figure 13 and plotted as a function of Δyear. As can be clearly seen there is a dichotomy in the distribution of angle values. The reason for this is that the observations span the period of WFPC2 history where two distinct focal plane solutions were used. The change to a different focal plane solution via a realignment of the Fine Guidance Sensor 1 (FGS1) resulted in the Science Instrument Aperture File (SIAF) being updated and this was on or about 1997.34. The large angles span a large enough time frame such that the compared source lists (not the reference source list) have observations dates that precede 1997.34 and the reference lists all have observation dates that occur after 1999.45. As a result the observations that generated the paired source lists have two different focal plane solutions and it could be that in the *idctab* reference file the information to correct for the two focal plane solutions was not propagated correctly. This has only been found in WFPC2 data so far. For the small angle measurements the dates of the compared source lists all have observation dates from 1996.05 to 1996.42 and 1997.42 to 2004.30. The reference source lists all have dates from 1996.06 to 1996.42 and 1997.44 to 2004.30. For the observations that created these paired source lists only one focal plane solution was used.

It can be inferred from Figure 13 that paired source lists that have a large Δyear value have large rotational offsets ($\geq 0.1''$). This, however, is an incorrect assumption. The reason for this is because all that needs to occur for a large rotational offset is for the observations to be taken with two different focal plane solutions. The boundary, as stated earlier, is 1997.34 and if observations are taken on either side of this boundary then there will be rotational offset that is $\geq 0.1''$. Note that the requirement of a large Δyear value as suggested by Figure 13 are not required because the only requirement is that both observations were taken on dates that cross the 1997.34 boundary.
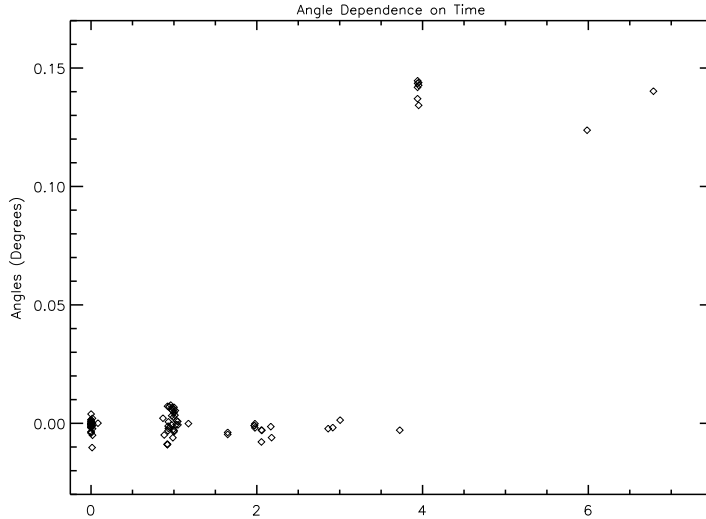
Fig. 13.— In this figure angles are plotted as functions of time differences. The abrupt increase in angle delineates the boundary in time where the solutions for the focal plane changed.

4.3. Differential Magnitudes

4.3.1. 0.10″ and 0.30″ Aperture Magnitudes

As opposed to the inspection of individual differential magnitudes, in this section all of the differential magnitudes are examined as a function of Δyear which is shown in Figures 14, 15, and 16 for the 0.10″ aperture magnitudes and in Figures 17, 18, and 19 for the 0.30″ aperture magnitudes. All of the figures reveal a slope that can originate in sensitivity, throughput, qauntum efficiency (QE), and/or charge transfer efficiency (CTE) losses with time. However, CTE losses are the dominant source of signal loss (Gonzaga, private communication). This will result in calculated magnitudes being fainter for more recent exposures than for earlier observations as these exposures will be less affected by CTE losses. The positive slopes derived from the linear fits in Figures 14, 15, 16, 17, 18, and 19 and the increasingly positive differential magnitude offsets do indeed imply that sensitivity, throughput, QE, and CTE losses have increased with time because in the paired source lists the reference source list is the more recent, while the compared source list is the earlier exposure. So when differential magnitudes are calculated the difference is taken as the reference magnitude subtracted from the compared magnitude resulting in a positive number that will increase in value as time progresses. This is because the reference magnitudes are increasingly affected by CTE losses, which make these reference magnitudes fainter as time evolves. Note that the magnitudes from the source lists have not been corrected for CTE losses. The slopes of the linear fits and the associated errors can be found in Table 5 and 6 for the 0.10″ and 0.30″ apertures,

21

respectively. Both tables have columns, which represent all filters, F606W, and F814W filters. The legend in the top plots in all of the figures have the the linear equation describing the Δyear dependence of the differential magnitudes.

A test was done to see if WFPC2 CTE is consistent with the linear equations derived from the differential magnitudes as a function of Δyear. The most accurate photometry is from the 0.30″ aperture and the largest Δyear is from data taken with the F814W filter. The linear equation from Figure 19 (see equation 1) was used as a check to see if CTE derived from the source list 8048_02 is consistent with the CTE calculated from the linear equation shown in Figure 19. The equation is presented for clarity:

$$\mathrm{dmag} \quad = \quad 0.0076345211\mathrm{x} - 0.00010328435 \tag{1}$$

where dmag is the differential magnitude, x is the Δyear and the slope has units of dmag/Δyear. Using a value of Δyear = 6.785302 the differential magnitude is 0.051699. Employing the WFPC2 CTE equations derived by Andrew Dolphin[3] and using a median flux value of $\approx 3088.22\mathrm{e}^-$ from the source list 8048_02 and a background of $\approx 17\mathrm{e}^-$ (derived from level 1 F814W data sets) the CTE in the y-direction is ≈ 0.080736. The differential magnitude of 0.051699 and the y-direction CTE of ≈ 0.080736 are consistent with each other suggesting that the slope of equation 1 is commensurate with the change in WFPC2 CTE as a function of time.

Another test was done to check the F606W filter of WFPC2. The linear equation tested in this case can be found in Figure 18 and is furnished in equation 2 for clarity:

$$\mathrm{dmag} \quad = \quad 0.012272440\mathrm{x} - 0.012582782 \tag{2}$$

where dmag is the differential magnitude, x is the Δyear and the slope has units of dmag/Δyear. Using a value of Δyear = 3.939576 the differential magnitude is 0.035765. Employing the WFPC2 CTE equations from Dolphin and using a median flux value of $\approx 3990.70\mathrm{e}^-$ from the source list 8090_if and a background of $\approx 10\mathrm{e}^-$ (derived from level 1 F606W data sets) the CTE in the y-direction is ≈ 0.067804. The differential magnitude of 0.035765 and the y-direction CTE of $\approx$ 0.067804 are consistent with each other suggesting that the slope of equation 2 is comparable with the change in WFPC2 CTE as a function of time. Furthermore, when inspecting the differences between the CTE values derived from both procedures it is discovered that the differences are essentially the same *i.e.,* the F814W difference is 0.029037 and the F606W difference is 0.032039.

[3]http://purcell.as.arizona.edu/wfpc2_calib/2008_07_19.html
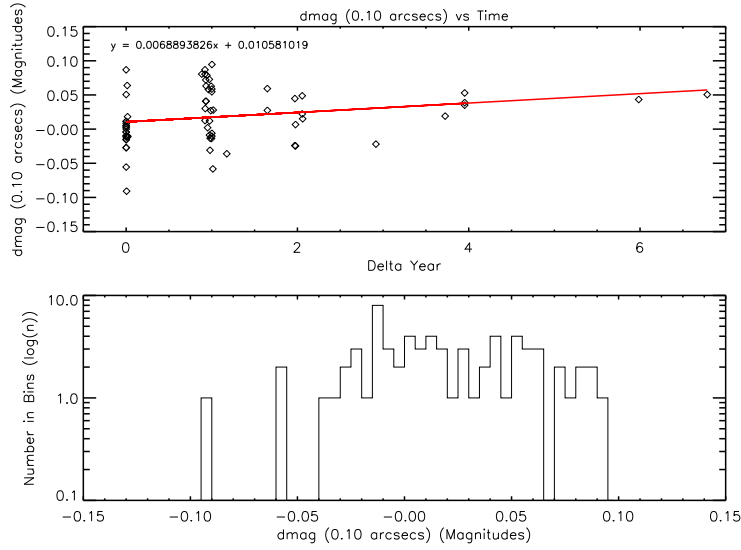
Fig. 14.— In this plot it is readily apparent that there is a time difference dependence on differential magnitudes, which can be seen in the top plot. The bottom plot is a histogram of the differential magnitudes. This plot includes all of the filters used in deriving the differential magnitudes at a $0.10''$ aperture.
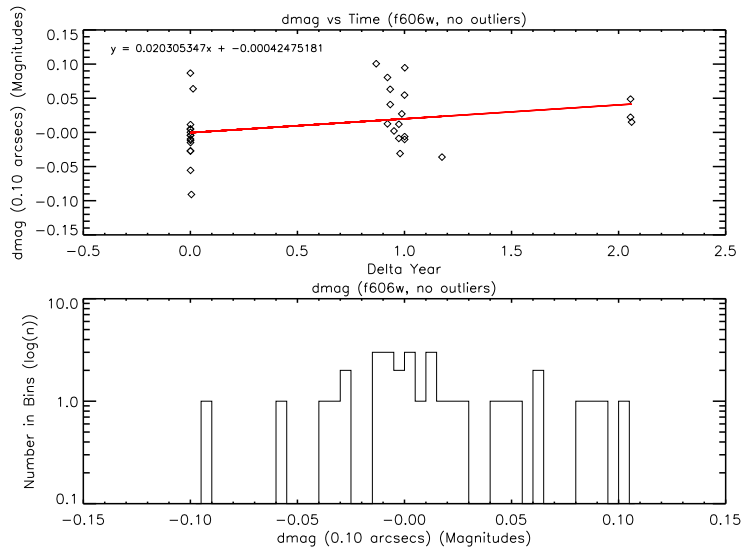

Fig. 15.— In this plot it is readily apparent that there is a time difference dependence on differential magnitudes, which can be seen in the top plot. The bottom plot is a histogram of the differential magnitudes. This plot includes only the F606W filter used in deriving the differential magnitudes at a $0.10''$ aperture.

23
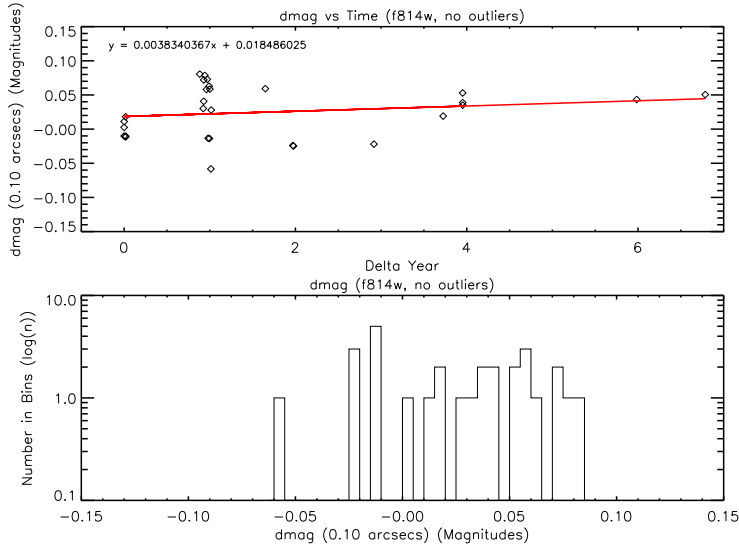
Fig. 16.— In this plot it is readily apparent that there is a time difference dependence on differential magnitudes, which can be seen in the top plot. The bottom plot is a histogram of the differential magnitudes. This plot includes only the F814W filter used in deriving the differential magnitudes at a $0.10''$ aperture.
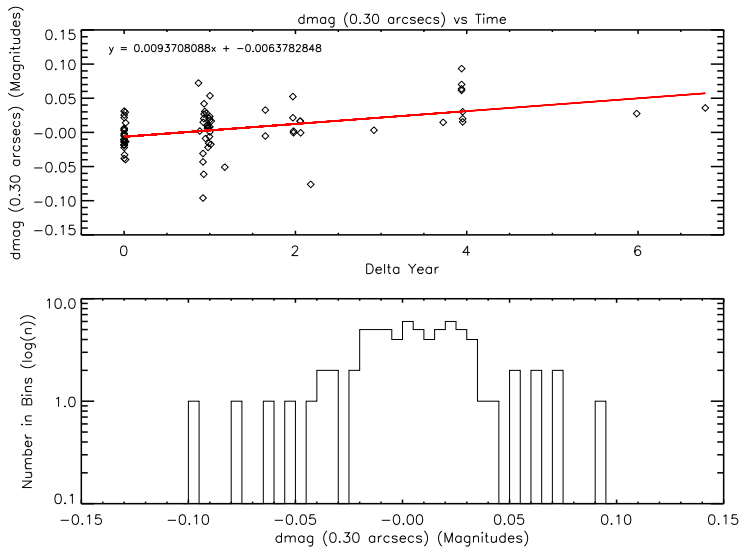
Fig. 17.— In this plot it is readily apparent that there is a time difference dependence on differential magnitudes, which can be seen in the top plot. The bottom plot is a histogram of the differential magnitudes. This plot includes all of the filters used in deriving the differential magnitudes at a $0.30''$ aperture.

24
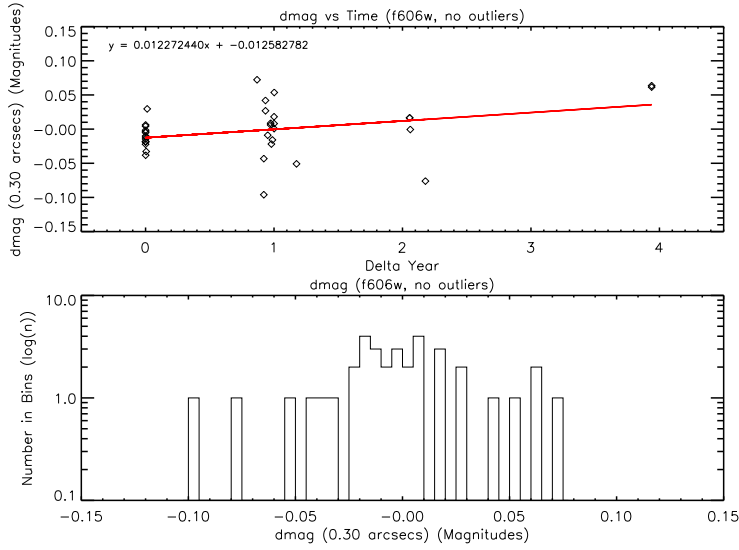
Fig. 18.— In this plot it is readily apparent that there is a time difference dependence on differential magnitudes, which can be seen in the top plot. The bottom plot is a histogram of the differential magnitudes. This plot includes only the F606W filter used in deriving the differential magnitudes at a $0.30''$ aperture.
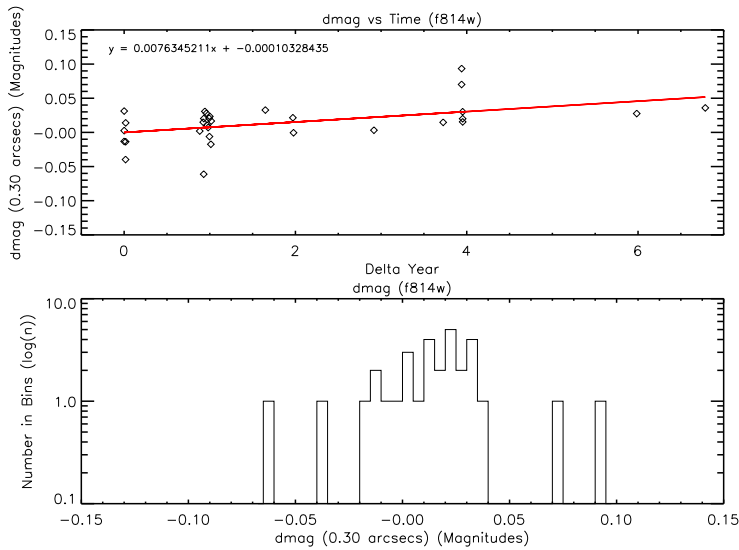
Fig. 19.— In this plot it is readily apparent that there is a time difference dependence on differential magnitudes, which can be seen in the top plot. The bottom plot is a histogram of the differential magnitudes. This plot includes only the F814W filter used in deriving the differential magnitudes at a $0.30''$ aperture.

Table 5: Slopes of Differential Magnitudes vs. Time Differences (0.10″ Aperture)

All Filters (dmag/Δyear)	F606W Filter (dmag/Δyear)	F814W Filter (dmag/Δyear)
0.0073 ± 0.0032	0.0207 ± 0.011	0.0045 ± 0.0035

Table 6: Slopes of Differential Magnitudes vs. Time Differences (0.30″ Aperture)

All Filters (dmag/Δyear)	F606W Filter (dmag/Δyear)	F814W Filter (dmag/Δyear)
0.0093 ± 0.0024	0.0121 ± 0.0054	0.0075 ± 0.0022

4.3.2. Differences in Slopes

The central reason why the slopes are not the same could be related to the different aperture sizes employed when deriving magnitudes but could also be that for F606W there are no time Δyear data points beyond 4. Since all magnitudes are put in the AB magnitude system the implication is that all magnitude offsets and aperture corrections should subtract out of the calculation leaving only instrument characteristics as the cause for differences in the slopes of the fitted lines. The main reason for the slope differences could be related to CTE losses. The larger aperture will gather more source and background counts but depending on how large or small the background is it will help to mitigate signal losses due to decreasing CTE. If the background is large then charge traps will be filled with counts from the background instead of filling the charge traps with signal from sources. On the other hand, however, if the background is small compared to the signal then the charge traps are filled with more signal counts due to the fact that there are less background counts to fill charge traps. Assuming that the backgrounds for the individual exposures are approximately the same then the source counts will fill the rest of the charge traps and that larger apertures should help mitigate some CTE losses as there are more counts that can be lost. If the backgrounds are not similar then this complicates the issue since any background mitigation of CTE will vary from observation to observation. Another aspect to keep in mind is that the CTE degrades over time and larger Δyear values should represent larger changes in the CTE than for Δyear values that span shorter times. This could be the reason for seeing the slopes increase for all filters and the F814W filter (see Tables 5 and 6, first and last columns). However, for the F606W filter there are no data Δyear value of 6 or greater. The largest Δyear value is 4, so perhaps the change in slope observed for F606W (see tables 5 and 6, second column) is related to not having any data points for Δyear values of greater than 4. Data points at Δyear values of greater than 4 could bring the slopes to be more similar to the all filters and F814W slopes.

4.4. Outliers in Differential Magnitudes

Outliers have been defined as having mean values greater than or less than -0.1 and 0.1 differential magnitudes, respectively. Table 7 contains these large mean differential magnitude offsets and RMSs and the columns are: in the first column are the paired source lists, second and third columns comprise of mean differential magnitudes, and the fourth column houses the filter used in the observation. The "X" signifies that the offset is less than the absolute value of 0.1. Examination of the outliers will be done in sets based on the reference source lists, which are the first entries in column 1. Likewise, Figures 20, 21, and 22 will be used to help determine the voracity of the offsets in Table 7. Note that the legends in Figures 20, 21, and 22 all contain the same type of information namely: the instrument and filter incorporated, differential magnitude offset, proposal identifications and visit numbers of both the reference and compared source lists.

To start look at the paired source lists with the reference file 8090_if. As noted in Table 7 the $0.30''$ aperture mean differential magnitudes are less than the value of 0.1, while the $0.10''$ aperture mean differential magnitudes are much greater than 0.1. Analysis of Figure 20's top plot reveals that the distribution of data around the mean is fairly even giving credence to the value of the mean differential magnitude offset. There are magnitude ranges (24.5 to 25.0 above the mean and 25.0 to 25.8 below the mean) where most of the points lie above or below the mean but these points negate each others contributions to either increasing or decreasing the mean. Scrutiny Figure 20's bottom plot, a histogram, signifies that the peak of the distribution is ≈ 0.22.

The next set of paired source lists to explore have the reference file 9677_m0. As shown in Table 7 both apertures have mean differential magnitudes that are greater than the absolute value of 0.1. Figure 21 has the plots of differential magnitudes and a histogram of the differential magnitudes. The top plot displays a distinct and odd shape for the distribution of data points and this therefore gives a robust measure of the mean differential offset. This same type of distribution can be found in the histogram of the bottom plot. The histogram clearly shows that a portion of the data is centered about 0, while other differential magnitudes range from $\approx$ -0.05 to -0.80.

The last set of paired source lists have the reference file 7274_23. The mean differential magnitudes found in Table 7 are greater than 0.1. Inspection of Figure 22 shows that the data points are evenly distributed about the mean (red line in top plot) suggesting the calculated mean is accurate. The bottom plot shows this as well because the data pints are more or less evenly distributed about 0.2.

Analysis of subsets of the data points using the IDL procedure aper.pro, which does aperture photometry, reveals approximately the same differential magnitude as the offsets implying that DAOphot and the HLA pipeline are not the cause of the problem (Wolfe & Casertano 2011a).

Table 7: Outliers in Differential Magnitudes

Paired Source Lists	dmag 0.10″ Aper.	dmag 0.30″ Aper.	Filter
8090_if, 6251_3w	0.228 ± 0.133	X	F606W
8090_if, 6251_3x	0.233 ± 0.132	X	F606W
9677_m0, 9677_l2	-0.280 ± 0.279	-0.181± 0.176	F606W
9677_m0, 9677_l3	-0.305 ± 0.297	-0.216 ± 0.189	F606W
7274_23, 6251_3u	0.234 ± 0.142	X	F814W
7274_23, 6251_3v	0.183 ± 0.136	X	F814W
9710_vt,[a] 9709_nh[a]	0.087 ± 0.307	-0.022 ± 0.123	F606W

[a] These particular data sets are designated an outlier because of the shape of the differential magnitude distribution is odd in magnitude space. See Figure 23.
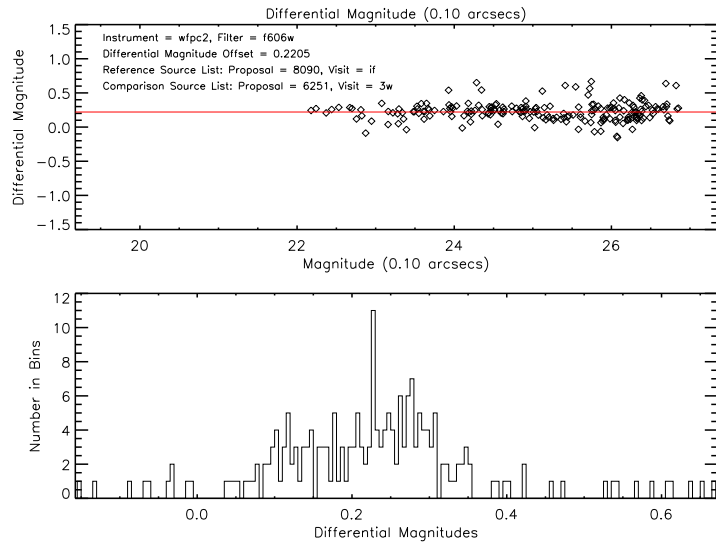
Fig. 20.— This is a plot of differential magnitudes with the mean overlaid as a red line shown in the top plot. The bottom plot shows a histogram of the differential magnitudes.
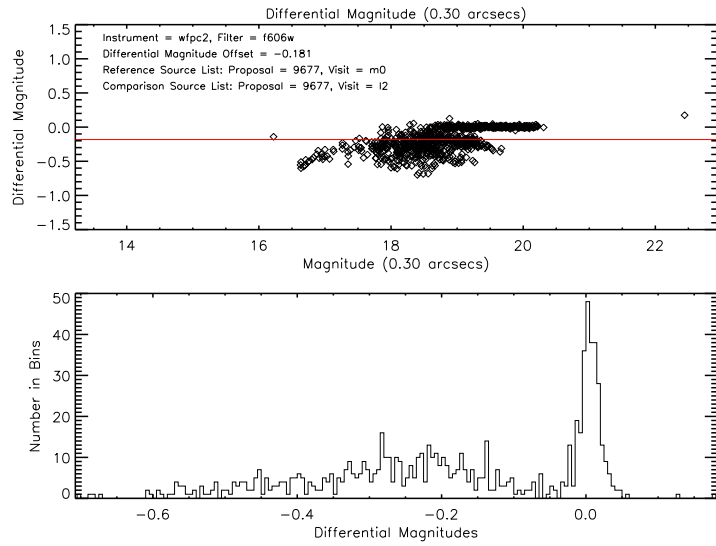
Fig. 21.— This is a plot of differential magnitudes with the mean overlaid as a red line shown in the top plot. The bottom plot shows a histogram of the differential magnitudes.
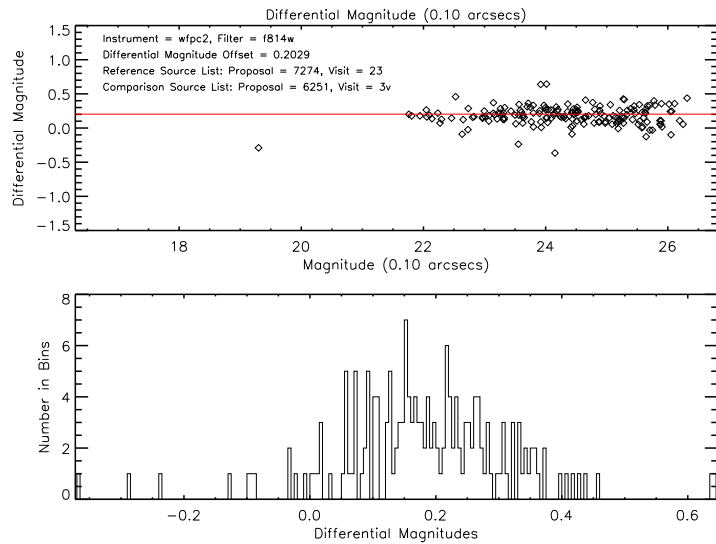
Fig. 22.— This is a plot of differential magnitudes with the mean overlaid as a red line shown in the top plot. The bottom plot shows a histogram of the differential magnitudes.
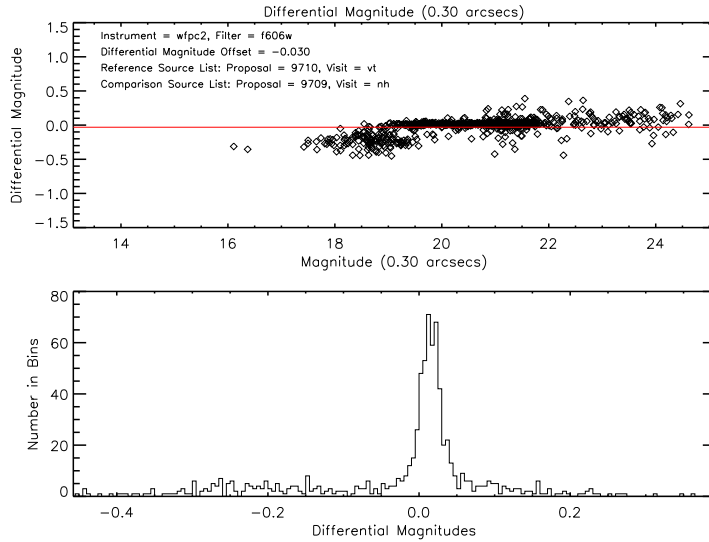
Fig. 23.— This is a plot of differential magnitudes with the mean overlaid as a red line shown in the top plot. The bottom plot shows a histogram of the differential magnitudes.

5. Conclusions

The examination of systematic properties of source lists as mentioned before is paramount when the product can be repeatedly used by a group of people. The preceding rigorous analysis supports the conclusion that the paired source lists are generated in a robust manner. The differential right ascension and differential declination show distinct distributions of data points that have large and small rotational offsets. Subsequently after the astrometric and rotational offsets have been eliminated the plots show random distributions centered around zero and have slopes associated with these distributions. This confirms that the algorithms employed to remove these offsets do this effectively. Because these offsets are removed efficaciously the result is that detector characteristics can be determined or at least estimated. Differential magnitudes communicate that the photometry is being accomplished robustly as well. The few outliers have been examined by reproducing the photometry, via an independent method, and have shown by calculating differential magnitudes that the problem does not lie with DAOphot but could instead be related to the observations themselves.

Investigation of all of the paired source lists together divulges information pertaining to the overall quality inherent in the paired source lists. To begin it is important to note that the astrometric offsets did not exceed $10''$ as the leeway in pointings within the paired source lists is $10''$. Astrometric offsets were derived "by hand" using the right ascension and declination obtained through HLA and when compared to the values derived by our algorithms it was found that they are essentially the same. Interestingly enough, examination of the angles determined between paired

30

source lists exemplifies that in using these analysis techniques it is possible to discover potential errors in reference files. It is also possible to see how CTE has caused magnitudes to decrease through interpretation of the dependence of differential magnitudes as a function of Δyear. As is readily apparent in the figures that demonstrate this dependence it is clear that for large time differences the differential magnitudes increase in value. Furthermore, CTE comparisons were made using Dolphin's CTE correction algorithms to derive CTE values and are consistent with the differential magnitudes values calculated from linear fits to differential magnitudes and Δyear. This implies that CTE, throughput, sensitivity, and QE losses (mainly CTE) are responsible for the differential magnitudes. Given that these losses are not taken into account in the generation of the $0.10''$ and $0.30''$ aperture magnitudes within the paired source lists it can be implied that the creation of the individual source lists is done in a consistent manner. Additional investigation needs to be done in order to achieve a full analysis of source lists generated not only by DAOphot but with SExtractor as well. Furthermore, since these analysis techniques are excellent in the investigation of detector characteristics it is therefore possible to discern relationships between the various instruments on HST and to map any changes that are revealed.

6.   Acknowledgements

7.   References

Bertin, E. & Arnouts, S. 1996, A&AS, 117, 393

Oke, J. B. & Gunn, J. E. 1983, ApJ, 266, 713

Pier, J. R., Munn, J. A., Hindsley, R. B., Hennessy, G. S., Kent, S. M., Lupton, R. H., & Ivezic, Z. 2003, AJ, 125, 1559

Skrutskie, M. F. et al., 2006, AJ, 131, 1163

Stetson, P. B. 1987, PASP, 99, 191

Wolfe, M. A., & Casertano, S., 2011a, HLA Document, "An Examination of the Large Mean Differential Magnitudes from Source Lists for WFPC2 and ACS Derived from DAOphot and SExtractor " (Baltimore: STScI)

Wolfe, M. A., & Casertano, S., 2011b, HLA Document, "An Examination of the Systematic Properties of Source Lists for WFPC2 and ACS Derived from SExtractor " (Baltimore: STScI)

8. Appendix

8.1. ΔPlate Scale (First Order Approximation)

This section shows mathematically how to derive to a first order approximation a change in the plate scale from two source lists that are separated in time. First start with the basic equations for x, y, x', and y':

$$x = x \tag{3}$$
$$y = y \tag{4}$$
$$x' = Sx \tag{5}$$
$$y' = Sy \tag{6}$$

where x and y are coordinates that are not scaled, whereas x', and y' are scaled quantities and S is the scaling factor. Now Δx and Δy are formulated in the following equations:

$$\Delta x = x' - x \tag{7}$$
$$= Sx - x \tag{8}$$
$$= x(S - 1) \tag{9}$$

and

$$\Delta y = y' - x \tag{10}$$
$$= Sy - y \tag{11}$$
$$= y(S - 1) \tag{12}$$

Now let:

$$x = \alpha \tag{13}$$
$$y = \delta \tag{14}$$
$$\Delta x = \Delta \alpha \tag{15}$$
$$\Delta y = \Delta \delta \tag{16}$$

where α is right ascension, $\Delta \alpha$ is the difference in right ascension from paired source lists, δ is the declination, and $\Delta \delta$ is the difference in declination between two source lists. Therefore equations 9 and 12 can be re-written using equations 13 through 16 as:

$$\Delta \alpha = \alpha(S - 1) \tag{17}$$
$$\Delta \delta = \delta(S - 1) \tag{18}$$

and rearranging:

$$\frac{\Delta \alpha}{\alpha} = (S - 1) \tag{19}$$
$$\frac{\Delta \delta}{\delta} = (S - 1) \tag{20}$$

Now to calculate the first order approximation of Δplate scale the average of the two slopes from plots of $\Delta\alpha$ vs. α and $\Delta\delta$ vs. δ are calculated. The equational form of this relationship can be found below:

$$\Delta\text{plate scale} = \frac{\frac{\Delta\alpha}{\alpha} + \frac{\Delta\delta}{\delta}}{2} \tag{21}$$

Equations 19 and 20 can be substituted into equation 21 to derive:

$$\Delta\text{plate scale} = \frac{(S-1) + (S-1)}{2} \tag{22}$$

$$= \frac{2(S-1)}{2} \tag{23}$$

$$= S - 1 \tag{24}$$

It is interesting to note that Δplate scale can also be calculated from equations 19 and 20 assuming that the plate scale is the same for right ascension and declination. If the plate scale for right ascension and declination are different then this implies that:

$$S \neq S' \tag{25}$$

This further suggests that S' can be either the negative of S and/or some multiple of S or both at the same time. Equations 19 and 20 can then be written as:

$$\frac{\Delta\alpha}{\alpha} = (S-1) \tag{26}$$

$$\frac{\Delta\delta}{\delta} = (S'-1). \tag{27}$$

A result of $S \neq S'$ is that the plate scale is not same for α and δ and this will introduce a skew between the α plate scale and the δ plate scale. The skew between plate scales is related through the difference in the plate scales:

$$\text{skew (plate scale)} = \frac{\Delta\alpha}{\alpha} - \frac{\Delta\delta}{\delta} \tag{28}$$

$$= (S-1) - (S'-1) \tag{29}$$

$$= S - S' \tag{30}$$

8.2. Rotation

This section derives how to calculate the rotation between paired source lists. First start with transformation equations:

$$x = x \tag{31}$$

$$y = y \tag{32}$$

$$x' = x\cos\theta - y\sin\theta \tag{33}$$

$$y' = x\sin\theta + y\cos\theta \tag{34}$$

where x and y are coordinates that are not rotated, whereas x' and y' are rotated quantities with respect to x and y and $\cos\theta$ and $\sin\theta$ are the rotation factors, while θ is the angle between the paired source lists. Now Δx and Δy are formulated in the following equations:

$$\Delta x = x' - x \tag{35}$$
$$= x\cos\theta - y\sin\theta - x \tag{36}$$
$$= x\cos\theta - x - y\sin\theta \tag{37}$$
$$= x(\cos\theta - 1) - y\sin\theta \tag{38}$$

and

$$\Delta y = y' - y \tag{39}$$
$$= x\sin\theta + y\cos\theta - y \tag{40}$$
$$= x\sin\theta + y(\cos\theta - 1) \tag{41}$$

now using the small angle approximation:

$$\cos\theta \approx 1 \tag{42}$$
$$\sin\theta \approx \theta. \tag{43}$$

Substituting equations 42 and 43 into equations 38 and 41 thereby producing the following results:

$$\Delta x \approx -y\theta \tag{44}$$
$$\Delta y \approx x\theta \tag{45}$$

and furthermore substituting equations 13 through 16 into equations 44 and 45 it is easy to see the dependence on right ascension and declination. The new equations are:

$$\Delta\alpha \approx -\delta\theta \tag{46}$$
$$\Delta\delta \approx \alpha\theta \tag{47}$$

and rearranging to show the slope as a function of rotation angle

$$-\frac{\Delta\alpha}{\delta} \approx \theta \tag{48}$$
$$\frac{\Delta\delta}{\alpha} \approx \theta. \tag{49}$$

Furthermore, if $\frac{\Delta\alpha}{\delta}$ and $\frac{\Delta\delta}{\alpha}$ have the same sign then a measure of the perpendicularity (another type of skew) between the right ascension and declination axes and can be found using the following equations:

$$\text{skew (non} - \text{perpendicularity)} = \frac{\frac{\Delta\alpha}{\delta} + \frac{\Delta\delta}{\alpha}}{2} \tag{50}$$

or

$$\text{skew (non} - \text{perpendicularity)} = \frac{-\frac{\Delta\alpha}{\delta} + -\frac{\Delta\delta}{\alpha}}{2} \tag{51}$$